Heliyon 10 (2024) e26972

Contents lists available at ScienceDirect

Heliyon

journal homepage: www.cell.com/heliyon

Research article

Experimental study on shearer traction vibration considering attitude disturbances

Dejian Ma [a,b], Lirong Wan [a,*], Qingliang Zeng [a], Zhaosheng Meng [a,c], Kuidong Gao [a], Jinwei Wang [a]

[a] College of Mechanical and Electronic Engineering, Shandong University of Science and Technology, Qingdao, 266590, China
[b] College of Safety and Environmental Engineering, Shandong University of Science and Technology, Qingdao, 266590, China
[c] State Key Laboratory of Mining Disaster Prevention and Control Cofounded by Shandong Province and the Ministry of Science and Technology, Shandong University of Science and Technology, Qingdao, 266590, China

ARTICLE INFO

Keywords:
Mining machinery
Shearer
Traction unit
Attitude disturbance
Vibration

ABSTRACT

Due to the influence of structural clearances, the shearer's oscillates and jumps concerning the scraper are frequent, which induces the collision and vibration impact of the traction components and exacerbates the traction failure of the shearer. Therefore, to explore the correlation between attitude disturbance and traction vibration, an experiment on the traction vibration is carried out, the spatial swaying of the shearer and vibration differences between two traction components are obtained, the influence of the lifting angle of the rocker arm is discussed, and the influence mechanism of the shearer attitude disturbance on traction vibration is elucidated. The results indicate that the rolling swing intensity of the shearer is the highest while the yawing swing intensity is the lowest, and the pitch swing intensity increases with the increase of the lifting angle of the rocker arm. Besides, the vibration impact indices of the two walking mechanisms have a competitive relationship of one decreasing but the other increasing, which can be used as a reference signal to judge the rolling swing and load-sharing performance of the traction part. Moreover, with the swing attitude, the competitive relationship of the average of vibration peaks is shown in the two support shoes, and it can be used as a reference signal to judge the pitching swing and the load-sharing performance of the traction part. This result reveals the impact mechanism of attitude disturbances on traction vibration and proposes a signal monitoring approach for judging the traction attitude disturbance and load-sharing performance, providing a reference for reducing traction faults.

1. Introduction

The high reliability of the fully mechanized mining equipment is an essential guarantee for efficient coal mining [1]. As the core equipment in mining face, the shearer has the drawback of structure asymmetric and unilateral traction drive, leading to the difficulty of maintaining spatial moment balance [2]. Besides, due to the large structural clearance and low positional constraint ability of the traction components, the shearer's oscillations and jumps concerning the scraper are frequent, which causes the spatial attitude disturbances of the shearer relative to the scraper machine. Under the influence of attitude disturbances, the hauling instability of the

* Corresponding author.
E-mail addresses: dejian_ma@sdust.edu.cn (D. Ma), lirong.wan@sdust.edu.cn (L. Wan).

https://doi.org/10.1016/j.heliyon.2024.e26972
Received 27 November 2023; Received in revised form 20 February 2024; Accepted 22 February 2024
Available online 28 February 2024

shearer reduces, the collision contact of the traction components and the traction vibration intensifies [3]. Attitude disturbance becomes an important factor in causing traction vibration and inducing traction failure. Additionally, the traction vibration caused by attitude disturbance is more than an important parameter for reflecting the traction characteristics of the shearer and the impact contact characteristics of traction components, it is also an important reason for the traction failure of the shearer. Therefore, exploring the influence of the attitude disturbances on the traction vibration of the shearer has a positive significance in reducing traction faults and improving traction reliability.

The chainless traction system is commonly used in the nowadays shearers, and it is mainly composed of electric motors, gear transmission systems, sliding shoes, and walking wheels [4,5]. Based on the multi-body dynamics theory and finite element methods, relevant scholars systematically studied the contact characteristics, vibration patterns, fatigue life, and transmission stability of the traction part of the shearer [6–8]. Xue et al. [9] established a mechanical analysis model of the whole shearer, and the small deformation coordination principle was introduced to solve the solution problem of over-constrained during the supporting of the shearer by four shoes. Zhang et al. [10] established a dynamic model for a three-drum shearer and studied the influence of structural parameters on the vibration mode. The results showed that the oil cylinder vibration amplitude of the front rocker arm reached 2.3 mm, while the rear rocker arm and middle rocker arm were 1.8 mm and 1.4 mm, respectively. With the objective functions of the coal loading rate, cutting ratio energy consumption and cutting load, Liu et al. established an optimization model for the traction speed of the shearer, providing a theoretical reference for achieving collaborative control between the cutting units and the traction units [11]. Based on friction and wear tests, Jaskowiec et al. [12] analyzed the adhesive wear, three body wear and fatigue wear mechanisms of the hauling wheel and the rail, and emphasized that the wear rate in the rail bending area is 2.5 times higher than that in the straight area. Kotwica et al. [13]reported a new track in the chainless traction system that mitigates hauling wheel tooth profile failure. The experimental test results showed that the new type of toothed track improves the traction stability of the shearer, reduces traction vibration more than two times, and reduces the wear volume by 35%. Considering the motion attitude, Zhang et al. [14] established a nonlinear multi-body dynamics system model of the shearer and analyzed the effects of equivalent elasticity-damping coefficient, rocker arm angle, and cutting load on the system vibration. The results showed that the vibration period of the system was prolonged with the increase of the equivalent stiffness of the hydraulic cylinder. Based on the wavelet denoising and independent component analysis, Ding et al. [15] proposed a nonlinear signal blind source separation and fault feature identification method, which was experimentally verified to be able to separate the vibration source of the shearer faults from nonlinear mixed signals and to be able to identify the vibration features of the shearer's fault at the early stage. Sun et al. [16] established the electromechanical coupling model of the shearer cutting unit, and they analyzed the influence of rocker height and hydraulic system on the vibration of the shearer. The results show that the drum height does not directly affect the shearer vibration but the pressure change of the hydraulic cylinder aggravates the shearer vibration. Gao et al. [17] found the cause of broken teeth of the shearer driving gear through the analysis of the fracture mechanism. Based on material optimization, tooth fillet trimming, and heat treatment process improvement, they proposed a method to improve the life of the driving gear. Considering the excitation of load frequency, Du et al. [18] established a torsional vibration model of the shearer's drive system, and they emphasized that the combined resonance caused by multi-frequency load exacerbates the torsional vibration and fatigue damage.

Besides, the research on the shearer position and pose detection mainly focuses on the shearer's positioning in the mining space. To eliminate accumulated time errors and improve positioning accuracy, Lu et al. [19] used multiple inertial navigation redundant positioning technology to build an experimental model with triple inertial navigation, and studied the influences of inertial navigation spacing and relative spatial angle. They pointed out that the inertial navigation spacing of 0.2 m and the horizontal installation can effectively improve positioning accuracy. Combining the positioning methods of inertial navigation, encoder, and laser radar, Wang et al. [20] proposed a multi-source information fusion positioning method for the shearer based on Kalman filtering, and they verified the feasibility of this method through experiments. With the aid of motion constraints and the magnetometer, Yan et al. [21] improved the stability and robustness of the shearer navigation system, and the navigation accuracy was improved by more than 70%. To improve the accuracy of the shearer positioning, Wu et al. [22] analyzed the shearer vibration and proposed an error correction method of the inertial navigation system, which effectively suppressed the impact of the vibration on the shearer positioning accuracy. By integrating the inertial guidance technology and fiber optic sensing technology, Feng et al. [23] constructed a spatial position relationship model between the hydraulic support, scraper and shearer, achieving a collaborative perception of the attitude among the three equipment. Meanwhile, the relative attitude relationship between the shearer and the scraper has attracted the attention of relevant scholars. The author's research team has successively analyzed the effect of the shearer's attitude disturbances on the meshing contact of the walking wheels [24,25]. And, some scholars have innovatively used the attitude information of the shearer body and sliding shoes to calculate the scraper attitude information [26], providing a reference for the study of the relative attitude disturbance characteristics of the shearer.

Scholars have conducted extensive research on the positioning and navigation of the shearer in the spatial coordinates of the mining space. However, the swaying and jumps between the shearer and the scraper are drastic, which is rarely reported in existing literature. The relative attitude disturbances between the shearer and scraper are often neglected in existing research. Besides, relevant scholars have accumulated a large number of innovative achievements in the traction dynamics of the shearer and proposed many effective methods to suppress the traction vibration. However, the interaction between the traction vibration and the attitude disturbances of the shearer relative to the scraper is not completely clear, which is not conducive to further revealing the collision contact mechanism of the traction components. Therefore, to reveal the correlation between attitude disturbance and traction vibration, experimental research on the traction vibration of the shearer is conducted in this article, and the traction vibration characteristics under the attitude disturbances of the shearer are investigated. The contribution of this study is to obtain the spatial swaying law of the shearer and the vibration differences between the traction components considering the structural clearance of the traction unit, and to

elucidate the influence mechanism of the shearer attitude disturbance on the traction vibration.

2. Materials and methods

Based on the principle of similarity, the shearer traction test system is constructed with reference to the structural parameters of the actual shearer and according to the scaling of 1:5, as shown in Fig. 1(a). In the traction test system, the center distance between the two walking wheels of the shearer is 1270 mm, the length of the rocker arm is 548 mm, the width of the shearer body is 320 mm, and the height of the shearer body is 310 mm, as shown in Table 1. The experimental system is equipped with seven multifunctional sensors, which communicate wirelessly with the computer through Bluetooth protocol, and it can simultaneously obtain information such as three-dimensional acceleration, spatial attitude angle, and angular velocity. The information transmission method of the testing system adopts Bluetooth wireless protocol, and the principle of the information collection and transmission is shown in Fig. 1(b). The sensor interacts with the human-machine interface host through Bluetooth protocol in a bidirectional manner, and then the human-machine interface host connects to the computer through a USB interface, finally, the signal display and sensor control are realized in the computer. The maximum designed hauling stroke of the shearer in the testing system is 2.5 m, which meets the usage range of the sensor's maximum wireless transmission distance of 10 m. The attitude disturbance and traction collision are different from high-frequency rotor systems, and their disturbance frequency is relatively low; additionally, the theoretical meshing frequency of a single tooth of the walking wheel is less than 3 Hz according to the design traction speed of 5 m/min. Therefore, the output frequency of the sensor at 100 Hz meets the actual testing requirements.

Sensor 1 and sensor 2 are respectively installed on the left and right support shoes for obtaining the vibration signals of the support shoes. Sensor 3 and sensor 4 are respectively installed on the outer side of the left and right traction boxes near the guide shoes and the end of the walking wheel shaft, for obtaining the vibration signals of the traction box and the swaying angle of the walking wheel. Sensor 5 is installed on the top of the shearer body and obtains the spatial attitude angle and angular velocity of the shearer, for the analysis of the shearer attitude disturbance. Sensors 6 and 7 are installed on the end faces of the left and right rocker arms to calibrate the lifting angle of the rocker arms. Sensors 1 to 4 are installed in a vertical position, with the x-axis pointing towards the traction direction, the y-axis pointing towards the vertical direction, and the z-axis pointing towards the goaf along the walking wheel axis. Sensors 5 to 7 are installed in a horizontal position, with the x-axis pointing towards the traction direction, the y-axis pointing towards the goaf side, and the z-axis pointing towards the vertical direction. The sensors are calibrated and the attitude angle is zeroed, using the initial position of the shearer as a reference. At present, the simulation experiment of shearer cutting while hauling is very challenging, and the no-load traction experiment can achieve the purpose of the attitude disturbance analysis and vibration test. Therefore, to reduce economic costs and simplify the testing process, the simulation test adopts the method of no-load traction. In the experiment, the influence of hydraulic pressure ripple on the attitude disturbances is not considered. It is assumed that the scraper machine runs straight and is not affected by terrain undulations, the coal mining machine is pulling at a uniform speed, and the structure of the sliding shoes is intact and not affected by wear. For the convenience of data management and analysis, the coordinates of each sensor are unified through coordinate transformation after the data collection, where the x direction refers to the traction direction, the y direction refers to the vertical direction, and the z direction refers to the axial direction of the drum.

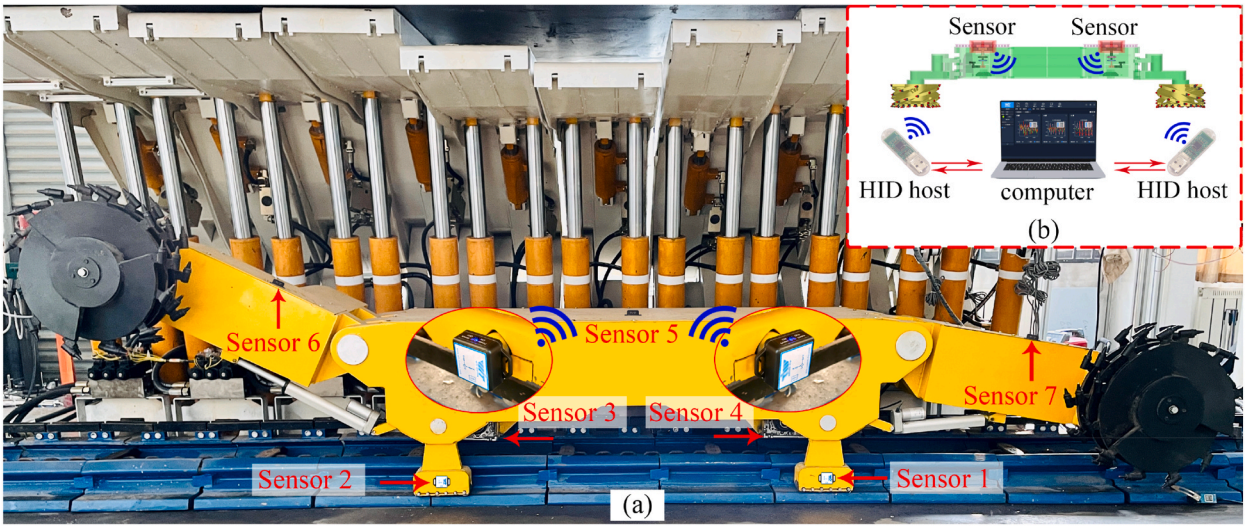

Fig. 1. The traction test system of the shearer: (a) test bench and sensor layout; (b) principle of signal acquisition.

Table 1
The comparison of the shearer structural parameters.

Structure parameter name	The actual shearer	Test system
Drum diameter	2500 mm	500 mm
The center distance of the walking wheel	6350 mm	1270 mm
The width of the shearer body	1600 mm	320 mm
The center of rotation of the rocker arm	8250 mm	1650 mm
The length of the rocker arm	2737 mm	548 mm
The length of the shearer body	1550 mm	310 mm

3. Results and discussion

3.1. The attitude disturbance analysis of the shearer

The angular velocity of the shearer attitude disturbances is obtained through the traction experiment, as shown in Fig. 2(a)-(c). The experiment results indicate that the shearer sways reciprocally around the three coordinates in space, which verifies the existence of the attitude disturbances between the shearer and the scraper. According to the experimental results, the effective values of the spatial swing angular velocity of the shearer are 5.4×10^{-2} rad/s, 8.2×10^{-3} rad/s, and 1.4×10^{-2} rad/s, respectively.

The roll swaying around the *x*-direction causes the support shoes and guide shoes to bear the support force alternately, inducing collision and impact on the bottom surface of the support shoes and the upper and lower groove surfaces of the guide shoes. And, the swaying around the *x*-direction is the main excitation cause of the rolling angle error of the walking wheels, which cannot be ignored for the torsional damage of the tooth body. Besides, the yaw swaying around the *y*-direction creates a yaw angle between the shearer and the scraper conveyor, and it causes the longitudinal loads to be carried alternately on the coal wall side and the goaf side of the guide shoes. This is an important cause for the impact contact on the lateral sides of the guide shoes. And, the swaying around the *y*-direction induces axial micro sliding on the tooth surface of the walking wheels, reducing the effective bearing tooth width. Moreover, the pitching swaying around the *z*-direction is the main reason for the upward lifting of the front haulage section while the downward pressing of the rear haulage section of the shearer. The swaying in the *z*-direction causes a pitch angle between the shearer and the scraper conveyor, which disrupts the load balance between the front and rear traction parts and affects the speed synchronization between the two traction parts. And, the pitching swaying is an important factor inducing the center jumping of the walking wheels, which exacerbates the impact damage on the tooth surfaces.

The special spatial structure is the critical cause to the torque instability of the shearer, and it induces spatial attitude disturbances, among which the asymmetric arrangement of the two rocker arms plays a decisive role. Therefore, to further explore the influence of the lifting angle of the rocker arm on the attitude disturbances, the box plots of the spatial swaying velocity of the shearer under different lifting angles of the left rocker arm are obtained through traction test, as shown in Fig. 3(a)-(c). In the experiment, the swing angle of the right rocker arm is calibrated as 12° using sensor 6, and the left rocker arm is calibrated as 32°–42° using sensor 7. The experimental results of the angular velocity show that the median of roll swaying is about 0 (Fig. 3(a)), and the median of yaw swaying and pitching swaying are −0.001 rad/s (Fig. 3(b)) and 0.003 rad/s (Fig. 3(c)), respectively. This indicates that, in the spatial swaying of the shearer relative to the scraper, there is a skewed distribution of yaw swaying and pitch swaying while the pitch swaying is the most significant. Among them, the skewed distribution of the yaw swaying is caused by the deviation of the drum from the *x*-axis of the machine body, while the skewed distribution of the pitching swaying is due to the upward trend on the left side of the shearer.

Meanwhile, to eliminate the interference of accidental factors on the attitude angular of the shearer, the maximum within the statistical range of 1%–99% is selected as the peak angular velocity of the shearer attitude, as shown in Table 2. The experimental results demonstrate that the roll swaying is significantly stronger than the yaw swaying and pitching swaying. This is because the center distance between the two guide shoes is large, which has a strong constraint on the yaw and pitching swaying of the shearer. On

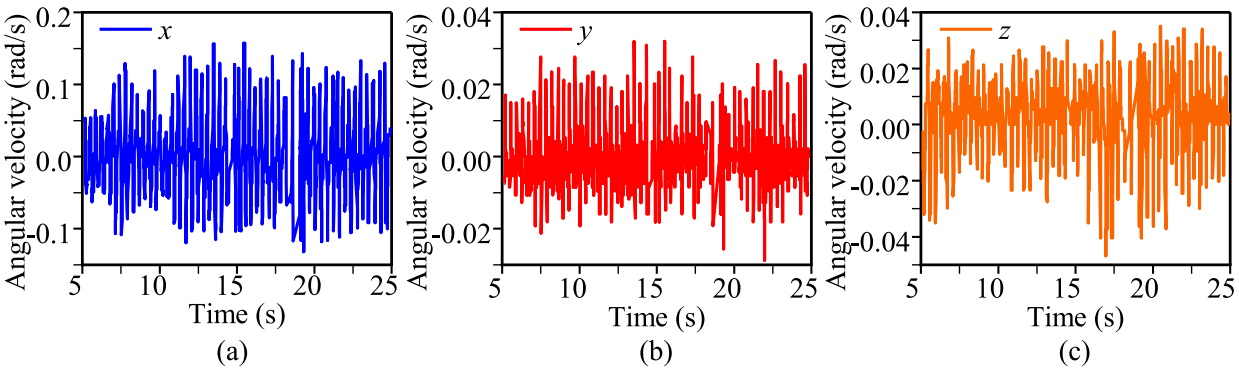

Fig. 2. The angular velocity of the attitude disturbance of the shearer: (a) around *x* direction; (b) around *y* direction; (c) around *z* direction.

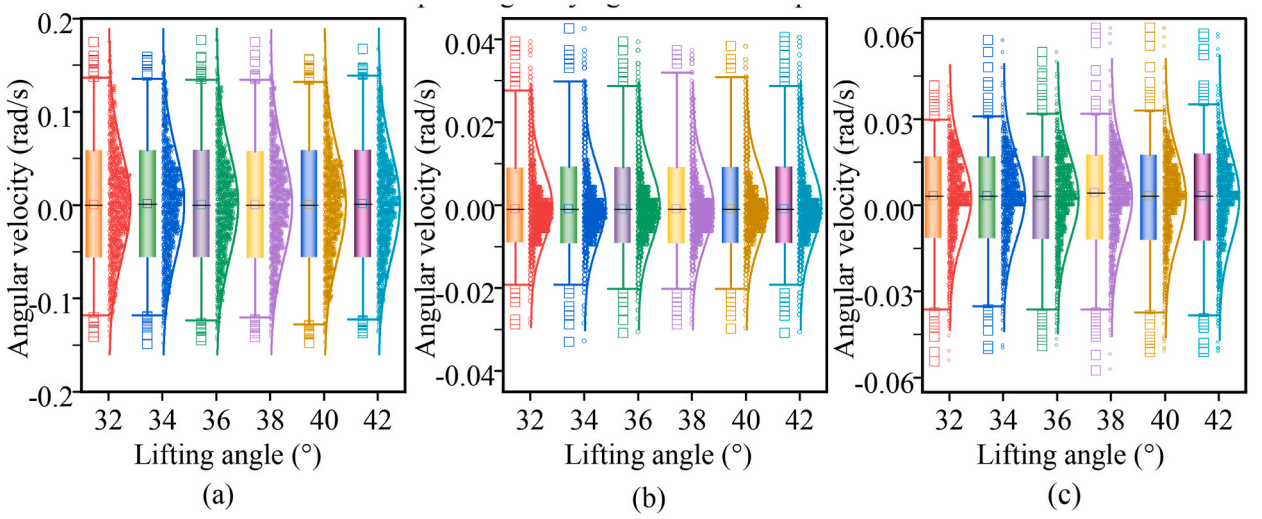

Fig. 3. The angular velocity of the attitude swaying of the shearer with different lifting angles of the rocker arm: (a) roll swaying; (b) yaw swaying; (c) pitching swaying.

Table 2
The peaks of the shearer angular speed under different rocker arm lifting angles.

Attitude swaying type	32°	34°	36°	38°	40°	42°
Rolling angular velocity rad/s	0.1364	0.1353	0.1342	0.1342	0.1342	0.1396
Yawing angular velocity rad/s	0.02770	0.02876	0.02876	0.02983	0.03089	0.02876
Pitching angular velocity rad/s	0.03621	0.03515	0.03621	0.03515	0.03728	0.03830

the other hand, the unilateral traction drive of the shearer exacerbates the roll swaying. The guide shoes are all located on the side of the goaf, but the support shoes on the side of the coal do not have the attitude constraint ability, making the constraint ability of the guide shoes to the rolling sway of the shearer weak.

To quantitatively analyze the influence of the rocker angle on the strength and impact performances of the shearer attitude swaying, the time-domain eigenvalues of the angular velocity of the shearer attitude are obtained from the experimental results, as shown in Figs. 4 and 5. Among them, the effective value of angular velocity R_{sm} is used to characterize the swaying strength, and the impact index F_{im} is used to characterize the impact performance of the shearer swaying, as shown in Equation (1)and Equation. (2):

$$R_{sm} = \sqrt{\frac{1}{N}\sum_{n=1}^{N} x_n^2} \tag{1}$$

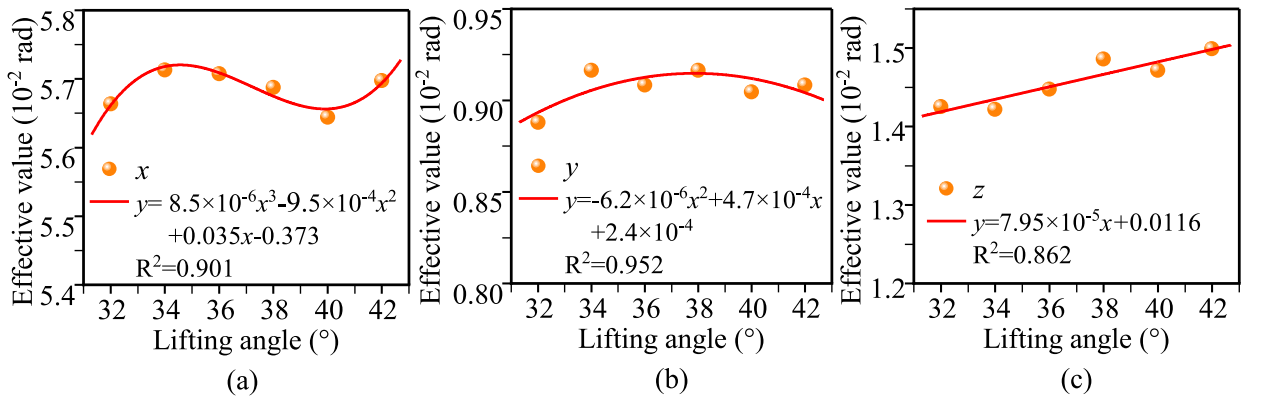

Fig. 4. The effective value of the shearer's swaying speed: (a) roll swaying; (b) yaw swaying; (c) pitching swaying.

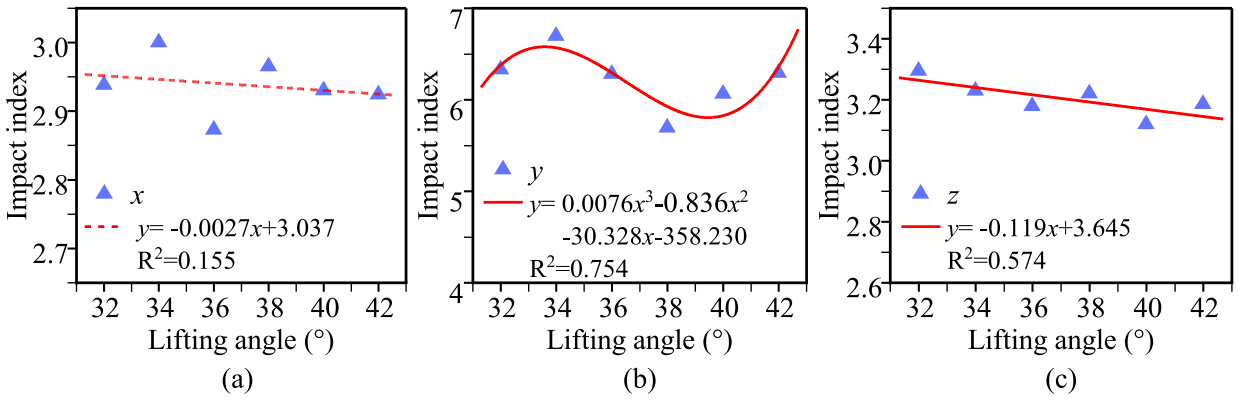

Fig. 5. The impact index of the shearer's swaying speed: (a) roll swaying; (b) yaw swaying; (c) pitching swaying.

$$F_{im} = \frac{max(|x_1|, |x_2|, |x_3| \ldots |x_N|)}{\frac{1}{N}\sum_{n=1}^{N} |x_n|} \tag{2}$$

As shown in Fig. 4(a)–(c), the effective value of the angular velocity and its correlation equation indicates that there is a good correlation between the swaying intensity of the shearer attitude and the lifting angle of the rocker arm, with correlation coefficients R^2 higher than 0.85. However, the correlation between the impact index of the angular velocity and the lifting angle is not significant Fig. 5(a)–(c). Among them, the pitching swaying intensity increases linearly with the increase of the lifting angle of the left rocker arm (Fig. 4(c)). This is because, the increase in the lifting angle of the left rocker exacerbates the tendency of the shearer with the front lifting and the rear sinking, which leads to the increase of the discontinuous collision contact of the front traction unit and the increase of the loading of the rear traction unit, and then increasing in the roll pitching intensity of the shearer. Besides, the roll swaying and yaw swaying have a nonlinear correlation with the lift angle of the rocker arm, and there are eigenvalues at 40° of the lifting angle (Fig. 4(a) and (b)). At this location, the overall swaying strength and impact property of the rolling disturbance and yawing disturbance are relatively low. This result provides a reference for adjusting and optimizing the angle of the rocker arm.

3.2. The vibration analysis of the walking mechanism

The vibration signal of the walking mechanism can directly reflect the collision contact impact of the walking wheels and the guide shoes. Therefore, in order to investigate the influence of the lifting angle of the rocker arm on the walking mechanism vibration and the contact impact of the guide shoes and the walking wheels, the vibration signals from sensors 3 and 4 are obtained respectively, with the lifting angle of the left rocker arm from 32° to 42°. Because the collision contact frequency of the guiding shoes induced by attitude disturbances is very low, and to focus on the influence of the lifting angle on the attitude disturbances and the vibration, low-pass filtering is adopted for the vibration signal, and the normal distribution statistics are shown in Fig. 6(a)-(f). The results show that the expected values of the vibrations of the left walking mechanism deviate from 0 in x and y direction, as shown in Fig. 6(a) and (b). Under the influence of the pitching swaying, the increase in the center distance of the left walking wheel and the intensification of the tooth top knocking are the reasons for the negative deviation of the x-direction vibration, while the increase in the contact clearance and the collisions on the guide shoe groove are the reasons for the positive deviation of the y-direction vibration.

To characterize the influence of the lifting angle of the rocker arm on the vibration intensity of the walking mechanism, the average value of the vibration peak is obtained according to the vibration signal, as shown in Table 3. The experimental results show that the size the and the overall increasing trend of the average vibration peak on the two walking mechanisms are basically consistent, indicating that the vibration strength of the walking mechanisms on both sides is basically the same. Also, as the lifting angle of the rocker arm changes, the overall trend of vibration intensity of the walking mechanisms on both sides is basically consistent. This indicates that the vibration intensity of the traction mechanism is mainly affected by the traction load and roll swaying, but it is less affected by the pitching swaying, and the collision contact between the side wall of the guide shoes and the pin rail is the main reason for the low-frequency vibration of the walking mechanisms. This analysis is supported by the experiment results in Table 3 where the z-direction vibrations of the walking mechanisms are the most significant.

To characterize the effect of the lift angle on the impact performance of the walking mechanism vibration, the vibration impact indexes are obtained according to the vibration signals, as shown in Fig. 7(a)-(f). The signal displays that the vibration impact property of the left side walking mechanism is higher than that of the right side, overall. The differences in vibration impact indexes between the two walking mechanisms are the result of the shearer's pitching swaying under the influence of the lifting angle. Combined with the analysis of Fig. 4(c), the increase of the left side of the shearer's upward tendency leads to the increase of the discontinuous impact contact on the left walking mechanism, and then the instantaneous collision impact is intensified; on the other hand, the increase of the right side of the shearer's downward tendency leads to the increase of the load-bearing strength on the right walking mechanism, and at the same time, the discontinuous impact contact is reduced and the instantaneous collision impact is weakened.

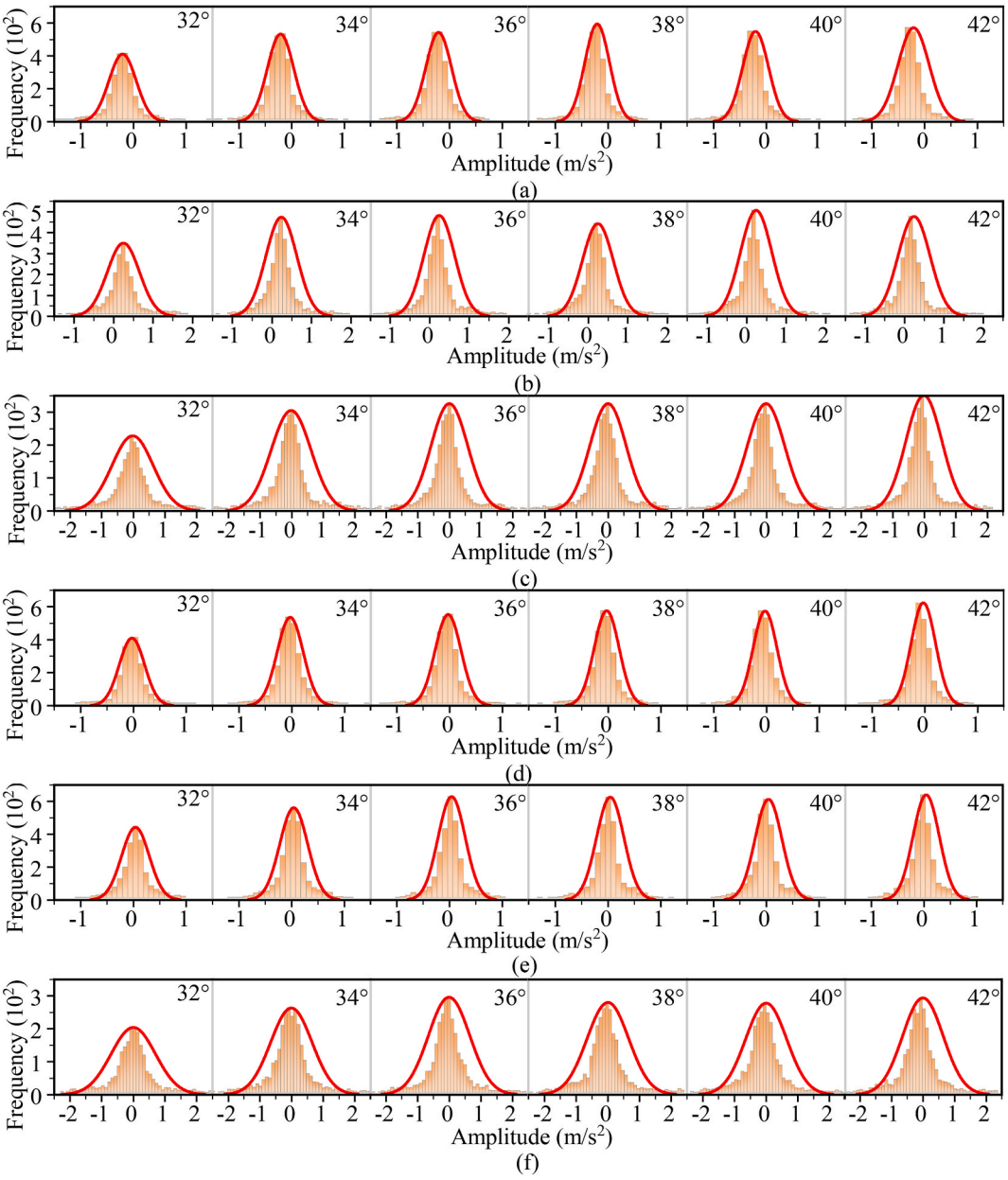

Fig. 6. The vibration statistics of the walking mechanism: (a) *x* direction of the left walking mechanism; (b) *y* direction of the left walking mechanism; (c) *z* direction of the left walking mechanism; (d) *x* direction of the right walking mechanism; (e) *y* direction of the right walking mechanism; (f) *z* direction of the right walking mechanism.

Table 3
The average value of the vibration peak of the walking mechanism.

Rocker arm lifting angle °	The left walking mechanism m/s^2			The right walking mechanism m/s^2		
	x	y	z	x	y	z
32	0.58463	1.20646	1.99907	0.61480	0.87671	2.10521
34	0.69882	1.17895	2.02742	0.71482	0.92070	2.03427
36	0.69763	1.18161	1.91668	0.71231	0.94006	2.15158
38	0.72191	1.15216	1.92005	0.68470	0.94177	2.14534
40	0.81005	1.19795	1.90894	0.74787	0.98281	2.06362
42	0.83014	1.21889	1.91885	0.74297	1.01791	2.05584

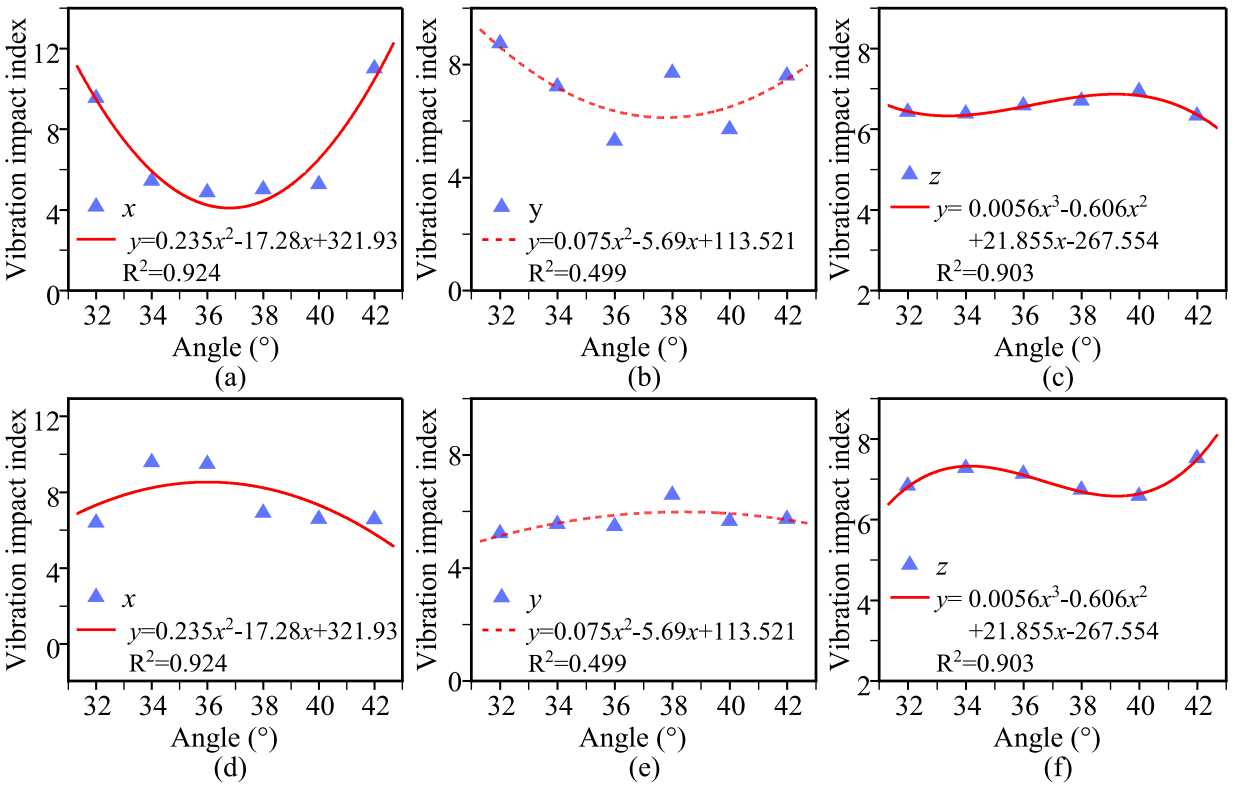

Fig. 7. The vibration impact index of walking mechanisms: (a) *x* direction of the left walking mechanism; (b) *y* direction of the left walking mechanism; (c) *z* direction of the left walking mechanism; (d) *x* direction of the right walking mechanism; (e) *y* direction of the right walking mechanism; (f) *z* direction of the right walking mechanism.

Furthermore, the experimental data indicates the vibration impact index of the walking mechanisms in the *x* and *z* directions are correlated with the lifting angle of the rocker arm, as shown in Fig. 7(a)–(c), Fig. 7(d) and (f). And the vibration impact index of the two walking mechanisms exhibits a clear competitive mechanism of one decreasing but the other increasing. On the one hand, combined with Figs. 4(a)–7(c) and (f), the *z*-direction vibration impact index of the left shoe is negatively correlated with the shearer roll swaying, while the *z*-direction vibration impact index of the right shoe is positively correlated with the shearer roll swaying. On the other hand, combined with Figs. 4(b)–7(a) and (d), the *x*-direction vibration impact index of the left shoe is negatively correlated with the shearer yaw swaying, while the *x*-direction vibration impact index of the right shoe is positively correlated with the shearer yaw swaying. Therefore, the roll swaying and yaw swaying of the shearer suppress the collision contact between the left guide shoe groove sidewall and the pin rail, but it further intensifies the collision contact between the right guide shoe groove sidewall and the pin rail. This is because the area of the left and right sides of the guide shoes groove is different, and the area near the coal wall is greater than the near on the goaf side. Under the combined action of the roll swaying and the yaw swaying, the left guide shoe is in contact with the pin rail on the goaf side, but the right guide shoe is in contact with the pin rail on the side near the coal wall, which is the reason for the vibration difference in the *z*-direction between the two guide shoes. Therefore, unlike the average value of the vibration peak, the difference in the vibration impact index between the two walking mechanisms can serve as a reference signal for determining the rolling swaying and the load-sharing characteristics between the two traction units of the shearer.

3.3. The vibration analysis of the support shoes

In order to further investigate the vibration characteristics of the support shoes under the shearer attitude disturbances, under different lifting angles of the rocker arm, the vibration signals of sensor 1 and sensor 2 are obtained respectively, as shown in Fig. 8(a)-(f). To obtain the time-domain characteristics of the vibration of the support shoes, based on the normal distribution statistics, the average value of the vibration peaks is obtained to characterize the influence of the lifting angle of the rocker arm on the vibration intensity of the support shoes, as shown in Fig. 9(a)-(f); and the vibration impact index is obtained to characterize the influence of the lifting angle on the impact performance of the support shoes' vibration, as shown in Table 4.

The experimental results show that the average vibration peaks and the vibration impact indexes of the left support shoe in three directions (Fig. 8(a)–(c)) are significantly higher than that of the right support shoe (Fig. 8(d)–(f)). This is because, caused by the disturbance of the pitching attitude of the shearer, the up and down oscillation of the traction units. Due to the asymmetric spatial structure, the shearer itself tends to tilt up on the front side, increasing in the structural clearance between the left support shoe and the

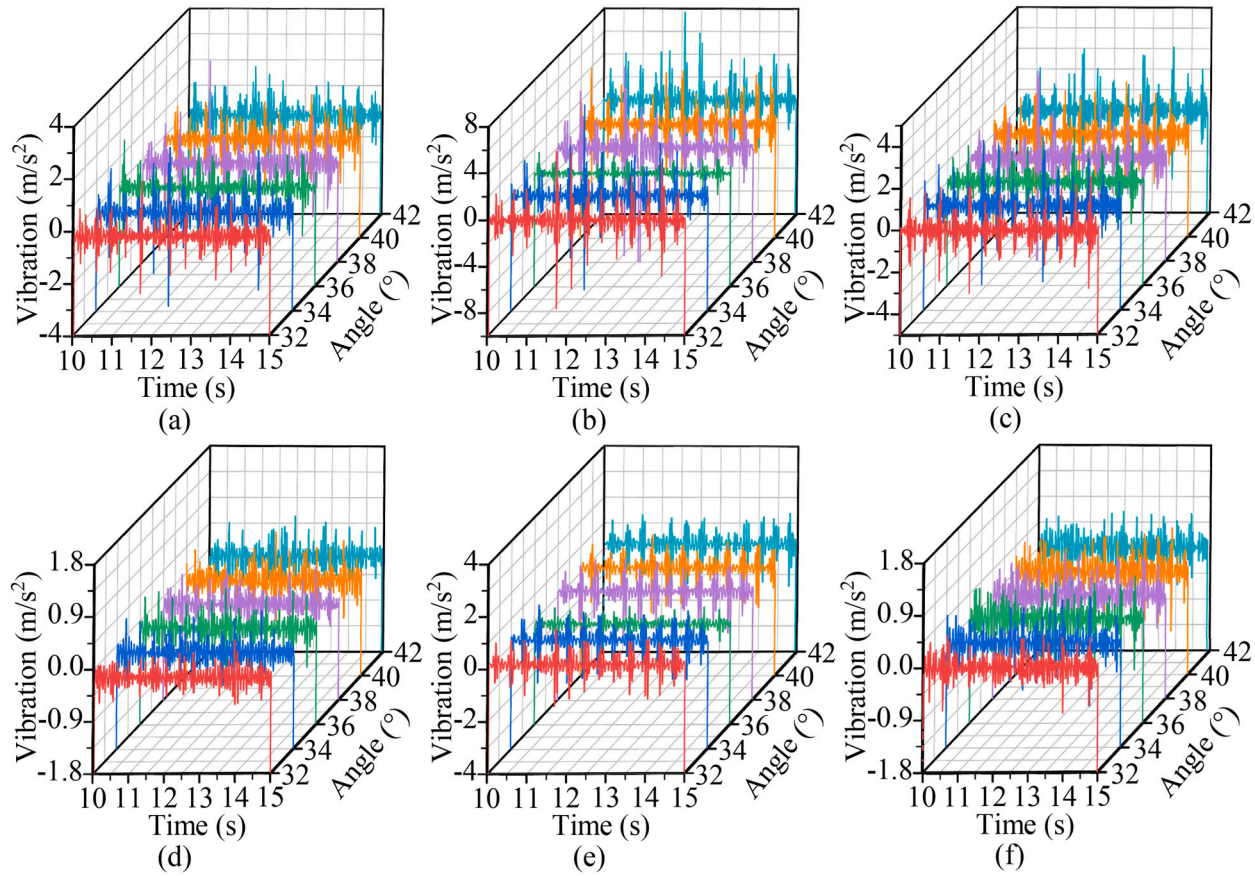

Fig. 8. The vibration characteristics of the support shoes: (a) *x* direction of the left shoe; (b) *y* direction of the left shoe; (c) *z* direction of the left shoe; (d) *x* direction of the right shoe; (e) *y* direction of the right shoe; (f) *z* direction of the right shoe.

scraper. At the same time, under the amplification effect of the pitching swaying attitude, the discontinuous collision contact between the left support shoe and the scraper further intensifies. Therefore, under the combined action of the structural clearances and the pitching swaying, the vibration intensity and the vibration impact property of the left support shoe are higher than those of the right shoe. This analysis is supported by the experimental results that the average value of the vibration peaks is the most significant in the *y* direction of the left shoe and the vibration impact index is the most significant in the *y* and *z* directions of the left shoe, as is shown in Fig. 9(a)–(f) and Table 4. The test results indicate that the left side of the shearer deviates upwards under the influence of the pitching swaying, which causes the bottom surface of the left support shoe hitting the scraper conveyor and the *y*-direction vibration of the left support shoe enhancing. This high cycle knocking phenomenon increases the pitting and fatigue wear on the bottom surface of the supporting shoes, which reduces the effective service life of the sliding shoe.

Besides, although there is no significant correlation between the vibration impact index of the support shoes and the rocker arm lift angles, there is a correlation between the average vibration peaks in the *x* and *y* directions and the rocker arm lift angles. The experimental data show that, with the rocker arm lifting angle increases, the average vibration peaks of the left support shoe decrease (Fig. 9(a) and (b)) while the average vibration peaks of the right support shoe increase (Fig. 9(d) and (e)). This is because, the increase in the lifting angle of the rocker arm leads to an increase in the pitching tendency of the shearer, and then the support load on the left support shoe reduces while the support load on the right support shoe increases.

Moreover, similar to the vibration impact indexes of the walking mechanisms, there is also an obvious competing mechanism between the average vibration peaks of the two support shoes with the change of the lifting angle. This vibration competition mechanism is mainly reflected in the *x* and *y* direction vibrations of the support shoes. Unlike the vibration of the walking mechanisms, with the strengthening of the pitching swaying, the vibration intensity of the left support shoe weakens while the vibration intensity of the right support shoe increases. Although the contact clearance of the left support shoe increases with the increase of the pitching swaying, the supporting load on the left support shoe decreases with the strengthening of pitching disturbance, which is the main reason for the decrease in the vibration intensity of the left shoe. Additionally, with the strengthening of the pitching swaying, the contact quality of the right support shoe improves but the supporting load on the right shoe increases, which is the main reason for the enhancement of the vibration intensity on the right support shoe. Therefore, the average value of the vibration peaks can reflect the pitching swaying attitude and the load-sharing characteristics of the supporting shoes on both sides, and it can be used as a reference

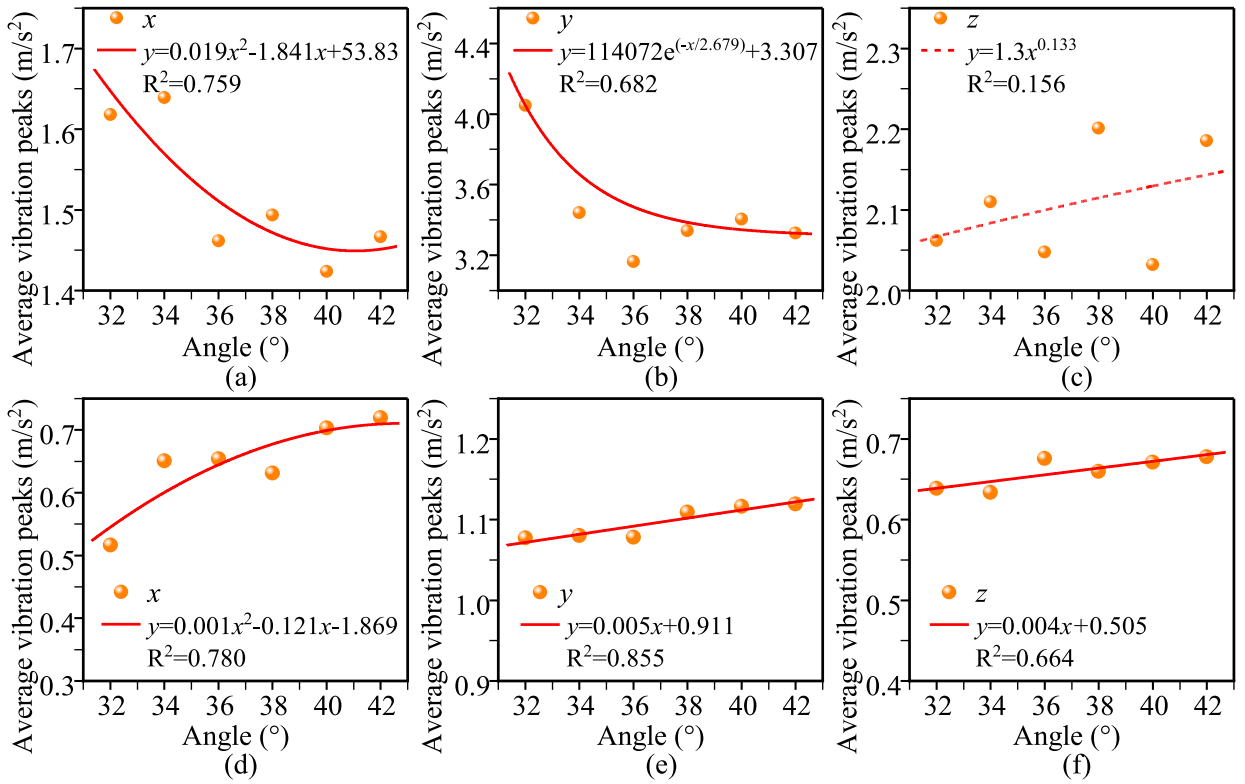

Fig. 9. The average value of the vibration peaks of support shoes: (a) *x* direction of the left shoe; (b) *y* direction of the left shoe; (c) *z* direction of the left shoe; (d) *x* direction of the right shoe; (e) *y* direction of the right shoe; (f) *z* direction of the right shoe.

Table 4
The vibration impact index of the support shoes.

Rocker arm lifting angle °	The left support shoe			The right support shoe		
	x	y	z	x	y	z
32	13.58452	12.48627	17.55932	5.24074	5.09526	5.79431
34	15.44369	17.55932	12.03040	4.75792	4.44602	5.94344
36	8.88111	10.24646	10.06312	5.64092	4.78334	5.93888
38	11.05564	15.29958	15.43614	4.49841	4.62150	5.28614
40	12.28118	13.50796	12.57412	4.35060	4.57979	5.39176
42	8.75232	11.76236	10.22744	5.35882	4.23634	5.62134

signal to determine the pitching swaying of the shearer and the load-sharing between the two traction units.

4. Conclusions

To explore the traction vibration characteristics of the shearer with the structural clearances and reveal the influence mechanism of attitude disturbances on traction vibration, a testing system for traction vibration of the shearer is established, the traction vibration laws of the shearer under the attitude disturbances are studied, and the influence of the rocker arm lifting angle is discussed. The research results are as follows:

1) The roll swaying disturbance of the shearer is obviously stronger than the yawing and pitching swaying disturbance, and the effective value of the angular velocity of the roll swaying is the largest while that of the yaw swaying is the smallest. Although the impact property of the attitude disturbances is not significantly correlated with the rocker arm lifting angles, the swaying intensity of the attitude disturbances has a better correlation with the lifting angle, and the swaying intensity of the pitching disturbance increases linearly with the increase of the left rocker arm lifting angle.
2) The vibration intensity of the walking mechanisms is mainly affected by the traction load and the rolling disturbance. The vibration impact indices of the two walking mechanisms have a competitive mechanism of one decreasing but the other increasing, which can be used as a reference signal to determine the shearer roll disturbance and the load sharing between the two traction units.

Besides, the rolling and yawing disturbances suppress the collision contact between the left guide shoe groove sidewall and the pin rail but intensify the collision contact of the right guide shoe.

3) The average value of vibration peaks and the vibration impact indexes of the left support shoe are significantly higher than those of the right support shoe. Besides, the average value of vibration peaks on the two supporting shoes also has a competitive mechanism, while the average vibration peaks of the left support shoe decrease overall but those of the right shoe increase overall as the lifting angle changes. Therefore, the average vibration peaks can be used as a reference signal to determine the shearer's pitching swaying and the load-sharing between the two traction units.

This study elucidates the influence of attitude disturbances on the traction vibration of the shearer, which is of positive significance in reducing traction failure. However, the effect of the time-varying load and terrain are not considered in the experiment. Therefore, the influence of the load characteristics under complex floor conditions and oblique cutting conditions on the shearer traction vibration is worth exploring in future research.

Data availability statement

Data can be shared on the request.

CRediT authorship contribution statement

Dejian Ma: Writing – review & editing, Writing – original draft, Visualization, Software, Methodology, Formal analysis, Conceptualization. **Lirong Wan:** Writing – review & editing, Project administration, Funding acquisition, Conceptualization. **Qingliang Zeng:** Writing – review & editing, Project administration, Funding acquisition. **Zhaosheng Meng:** Project administration, Funding acquisition. **Kuidong Gao:** Project administration, Funding acquisition. **Jinwei Wang:** Visualization, Software.

Declaration of competing interest

The authors declare that they have no known competing financial interests or personal relationships that could have appeared to influence the work reported in this paper.

Acknowledgements

This research was funded by the national natural science foundation of China (Grant No. 52174146, 52104164); the central government guides local funds for science and technology development (YDZX2022013).

References

[1] J. Brodny, M. Tutak, Applying sensor-based information systems to identify unplanned downtime in mining machinery operation, Sensors 22 (2022) 2127, https://doi.org/10.3390/s22062127.
[2] D. Ma, L. Wan, Z. Lu, X. Zhang, Q. Zeng, K. Gao, Research on the traction dynamic of shearer based on the pose analysis, Eng. Fail. Anal. 130 (2021) 105760, https://doi.org/10.1016/j.engfailanal.2021.105760.
[3] L. Boloz, Z. Rak, J. Stasica, Comparative analysis of the failure rates of shearer and plow systems-a case study, Energies 15 (2022) 6170, https://doi.org/10.3390/en15176170.
[4] X. Cheng, H. Yang, L. An, Strength analysis and tooth shape optimization design of the pin rail wheel of the shearer, Mach. Tool & Hydraul. 47 (2019) 114–120, https://doi.org/10.3969/j.issn.1001-3881.2019.06.020.
[5] J. Korski, Longwall shearer haulage systems - a historical review. Part 2 – First cordless haulage systems solutions, Min. Mach. 39 (2021) 24–33, https://doi.org/10.32056/KOMAG2021.2.3.
[6] X. Yang, Y. Zhang, X. Chen, Y. Wang, L. Zhao, X. Wang, G. Zhang, Study on wear behavior of coatings fabricated by additive manufacturing technology on the surface of guide shoe of shearer, J. Phys.: Conf. Ser. 2549 (2023) 012010, https://doi.org/10.1088/1742-6596/2549/1/012010.
[7] X. Li, Y. Guo, S. Han, Analysis of fault characteristics of planetary gearbox of shearer, in: Mechanisms and Machine Science, 2023, pp. 900–911, https://doi.org/10.1007/978-3-031-26193-0_79.
[8] L. Wang, D. Zhang, D. Wang, C. Feng, A review of selected solutions on the evaluation of coal-rock cutting performances of shearer picks under complex geological conditions, Appl. Sci.-Basel. 12 (2022) 12371, https://doi.org/10.3390/app122312371.
[9] J. Xue, S. Zhao, L. Yang, Research on key technology of digital modeling for ultra high mining shearer, Coal Sci. Technol. 47 (2019) 13–20.
[10] Q. Zhang, Y. Wang, B. Li, Y. Tian, Vibration analysis of a three-drum shearer for a large mining height, Strength Mater. 52 (2020) 160–170, https://doi.org/10.1007/s11223-020-00161-2.
[11] X. Liu, X. Li, X. Fu, X. Yang, J. Zhang, Analysis on the influence law of traction speed on the cutting performance of coal containing hard concretion, Mec. Ind. 24 (2023) 5, https://doi.org/10.1051/meca/2023001.
[12] K. Jaskowiec, Z. Pirowski, M. Glowacki, M. Bisztyga-Szklarz, A. Bitka, M. Malysza, D. Wilk-Kolodziejczyk, Analyze the wear mechanism of the longwall shearer haulage system, Materials 16 (2023) 3090, https://doi.org/10.3390/ma16083090.
[13] K. Kotwica, G. Stopka, A.N.N. Wieczorek, M. Kalita, D. Balaga, M. Siegmund, Development of longwall shearers' haulage systems as an alternative to the eicotrack system used nowadays, Energies 16 (2023) 1402, https://doi.org/10.3390/en16031402.
[14] X. Zhang, G. Yao, Y. Zhang, Nonlinear multi body dynamic modeling and vibration analysis of a double drum coal shearer, J. Cent. South Univ. 28 (2021) 2120–2130, https://doi.org/10.1007/s11771-021-4757-z.
[15] H. Ding, Y. Wang, Z. Yang, O. Pfeiffer, Nonlinear blind source separation and fault feature extraction method for mining machine diagnosis, Appl. Sci.-Basel. 9 (2019) 1852, https://doi.org/10.3390/app9091852.
[16] L. Sun, K. Jiang, Q. Zeng, K. Gao, X. Zhang, Influence of drum cutting height on shearer cutting unit vibration by co-simulation method, Int. J. Simulat. Model. 20 (2021) 111–122, https://doi.org/10.2507/IJSIMM20-1-548.
[17] T. Gao, Failure analysis and improvement measures of traction chain wheel of high-power shearer, Coal Sci. Technol. 50 (2022) 323–326.

[18] W. Du, W. Li, S. Jiang, L. Sheng, Y. Wang, Nonlinear torsional vibration analysis of shearer semi-direct drive cutting transmission system subjected to multi-frequency load excitation, Nonlinear Dynam. (2022), https://doi.org/10.1007/s11071-022-08041-x.
[19] C. Lu, S. Wang, K. Shin, W. Dong, W. Li, Experimental research of triple inertial navigation system shearer positioning, Micromachines 14 (2023) 1474, https://doi.org/10.3390/mi14071474.
[20] L. Wang, Accurate Positioning Method of Shearer Based on Multi-Mode Information Fusion, China University of Mining and Technology, Master, 2021, https://doi.org/10.27623/d.cnki.gzkyu.2021.000414.
[21] M. Yan, Z. Wang, Precise shearer positioning technology using shearer motion constraint and magnetometer aided SINS, Math. Probl Eng. 2021 (2021) 1–12, https://doi.org/10.1155/2021/1679014.
[22] G. Wu, X. Fang, L. Zhang, M. Liang, J. Lv, Z. Quan, Positioning accuracy of the shearer based on a strapdown inertial navigation system in underground coal mining, Appl. Sci.-Basel. 10 (2020) 2176, https://doi.org/10.3390/app10062176.
[23] H. Feng, X. Fang, N. Chen, Y. Song, M. Liang, G. Wu, X. Zhang, Research on the three-machines perception system and information fusion technology for intelligent work faces, Sensors 23 (2023) 7956, https://doi.org/10.3390/s23187956.
[24] D. Ma, L. Wan, X. Zhang, Q. Zeng, K. Gao, Meshing characteristics and failure analysis of shearer walking wheel considering torsional deformation, Alex. Eng. J. 61 (2022) 5771–5782, https://doi.org/10.1016/j.aej.2021.09.035.
[25] D. Ma, L. Wan, K. Gao, Q. Zeng, X. Wang, The meshing and failure analysis of haulage wheels with the effect by shearer's poses, Eng. Fail. Anal. 137 (2022) 106251, https://doi.org/10.1016/j.engfailanal.2022.106251.
[26] X. Zhang, Design and Implementation of Virtual Cooperative Operation System of Shearer and Scraper Conveyor under Complex Floor Conditions, Taiyuan University of Technology, Master, 2021, https://doi.org/10.27352/d.cnki.gylgu.2021.001174.